university of groningen

University Medical Center Groningen

University of Groningen

Improving the clinical applicability of laser Doppler perfusion monitoring

Morales, Fernando

IMPORTANT NOTE: You are advised to consult the publisher's version (publisher's PDF) if you wish to cite from it. Please check the document version below.

Document Version
Publisher's PDF, also known as Version of record

Publication date:
2005

[Link to publication in University of Groningen/UMCG research database](#)

A model for Post-Occlusive Reactive Hyperaemia, as measured with Laser Doppler Perfusion Monitoring

Frits F.M. de Mul, Fernando Morales, Andries J. Smit, Reindert Graaff

Summary

To facilitate the quantitative analysis of Post Occlusive Reactive Hyper-aemia (PORH), measured with Laser Doppler Perfusion Monitoring (LDPM) on extremities, we present a flow model for the dynamics of the perfusion of the tissue during PORH, based on three parameters: two time constants (τ_1 and τ_2) and the ratio of the maximum flux and the resting flux. With these three constants, quantitative comparisons between experiments will be possible, and therefore we propose to adopt this approach as future standard. For this reason we also developed a computer program to perform the fit of the model to measured data.

5.1 Introduction

Microcirculation is the blood flow through vessels smaller than 0.1 mm in diameter, the microvasculature. In the skin, its function is to provide nutrients and to allow exchange of gases and regulation of temperature. The regulation of the microcirculation is controlled by the musculature of the arterioles, which change the local tissue perfusion. The regulation is mostly due to changes in the ambient temperature or in the concentration of several substances like oxygen, carbon dioxide, nitric oxide, and others related to the metabolism. Endothelial function may also be a determinant of skin perfusion. If a decrease of blood flow occurs, the increase of waste products or decrease of oxygen levels will induce vasodilatation that will enhance blood flow until the normal situation is reached again. In healthy subjects, this regulation system is capable of increasing the perfusion at least tenfold compared to resting flow conditions [1]. However, in the case of Peripheral Arterial Obstructive Disease (PAOD) the presence of stenosis in proximal arteries will decrease the available pressure at the level of the arterioles. In that case, distal vasodilatation might be a proper reaction to prevent an increased concentration of waste products (i.e. carbon dioxide) and to supply enough oxygen in order to maintain the necessary metabolic condition.

The post-occlusive reactive hyperaemia (PORH) test has been proposed to assess the microvascular function. The local blood perfusion, e.g. at a distal extremity, is measured before, during and after performing arterial occlusion, to record the response upon releasing the occlusion. When the measurement is performed by means of a laser Doppler perfusion monitor (LDPM) a characteristic signal output is obtained similar to Figure 5.1. Upon occlusion, a PORH tracing shows that the blood perfusion drops from its resting flux value to the biological zero level [2]. After releasing the cuff the blood perfusion returns to the resting flux value, but with an overshoot. The magnitude and time regime of that overshoot are clinically relevant diagnostic variables [3,4].

In normal (healthy) cases, immediately after cuff release the flux will quickly rise to a maximum followed by a slower decrease to initial (resting flux) values. The reason for the increased flux after cuff release is mostly the vasodilatation due to the ischemia produced by the occlusion. Both endothelium-dependent and –independent effects might modulate the degree of vasodilatation. In the presence of proximal stenosis or obstruction (atherosclerosis), the peak perfusion value that occurs after occlusion will be relatively lower. In case of critical ischemia, the maximum vasodilatation has already been reached in the resting period, before occlusion, and

the PORH response will not show a higher response than that resting flux level. Also the increase of flux after occlusion will be smaller because of the presence of stenosis in the larger arteries, which will inhibit a rapid re-filling of the arterial segments.

The rate of flux increase just after cuff release is another important parameter, which is much lower in the case of PAOD. It is not only determined by the decreased vascular resistance of the capillaries and the arterioles, but also by the higher resistance of the larger arterial blood vessels and the volume increase of the (larger) arterial blood vessels distal to the occlusion cuff, which determine the refill of that blood vessel segment. It should be noted that the decreased rate of flux increase just after cuff release is not explained by decreased dilatation of the blood vessels. After the occurrence of the maximum flow, the oxygenation of the tissue normalizes, and the need for the hyperaemic response vanishes. At that time, the vasodilatation will decrease.

Previously, various models to describe the overall blood flow in the cardiovascular system have been published, but not for the capillary system. The cardiovascular models start from the early "Windkessel" model by Frank [5]. In its essence, this model consists of a resistance in series with the load impedance and a compliance (with a "capacitance" as the electrical analogue) parallel to it. This scheme will act as a first-order low-pass frequency filter, which means that its transfer of fast changes in the supply pressure ("voltage") will be considerably lower than that of slowly varying
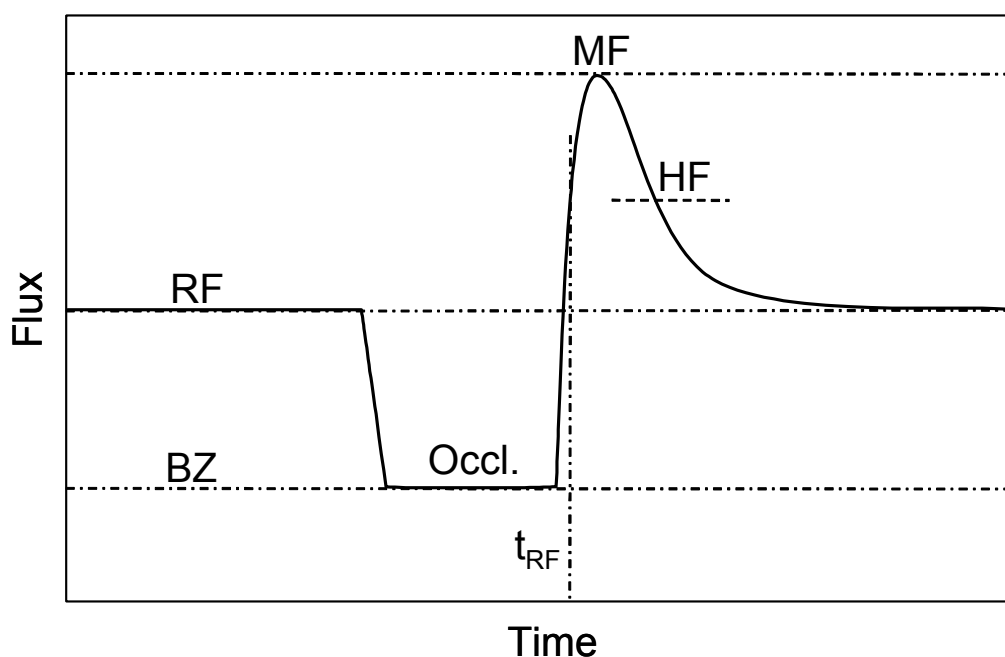

Figure 5.1. Post-Occlusive Reactive Hyperaemia (PORH) response. BZ = biological zero, Occl. = occlusion period, RF = resting flow, MF = maximum, HF = half decrease time between maximum and resting flux, t_{RF} = time of cross point with RF.

or constant pressures. Such a filter will transfer stepwise changes in pressure gradually and with some delay. For better matching with experimental data Westerhof [6] added a series resistance parallel to the compliance. Burattini c.s. [7] included an inertia part (an "inductance") in series or parallel to the series resistance, to take the flow inertia of the mass of blood in the vessel into account. In various publications, these circuits were then used as the basic blocks in building complex systems to describe the systemic blood flow through the heart, the organs, and the supplying vessels. See e.g. Geertsema et al. [8] or Ferrari et al. [9] and references therein.

However, for the capillary perfusion, as probed with LDPM, no such models have been published so far. A simplified model of the signals that can be obtained during reactive hyperaemia was published by Humeau c.s. [10] They used, following earlier studies by Smye and Bloor [11] and Wilkin [12], an exponentially increasing behaviour for the radius of the vessels during vasodilatation, and from this a similar function for the amount of erythrocytes passing by. For the period after vasodilatation they used a simple exponentially decreasing function. The simulated signals obtained with this model showed schematically the particular increase-decrease behaviour characteristic for the hyperaemia signals.

The aim of this study is to present a physical model to describe the total PORH response of LDPM signals in general and to determine the characteristic time constants and fluxes of the signal as depicted in Figure 5.1 in such a way that the influence of noise and signal fluctuations is diminished. The model is made such that comparisons between recordings of different patients, even when obtained in different laboratories, can be performed easily.

5.2   The PORH model

The physiological model, as described in the Introduction, may contain a time-varying flow resistance for the capillary part of the circulation. This resistance should have following characteristics:

- At the end of the occlusion, when releasing the cuff, the resistance of the capillaries should be small, since the arterioles are assumed to be wide open,

- During the hyperaemia period the resistance gradually should increase with decreasing diameters of the arterioles,

- There should be a parallel "leakage" resistance, to account for probable shunts inside or outside the capillary bed,

- Finally, the resistance should return to the value it had before the occlusion, i.e. the "resting flux" situation.

With this in mind we developed the model as shown in Figure 5.2. In this model, using the flow (assumed as proportional to the flux signal) expressed in [m³/s], V_0 and V_1 denote pressures [Pa = N/m²], $R_{cap}(t)$, $R_1..R_4$ denote flow resistances [Ns/m^5] and C_1, C_2 are compliances, expressed in [m^5/N]. The left and right parts of the circuit (left and right from V_1) account for the arterial and the capillary circulation part respectively. In the upper panel the capillary part first is represented by a time-varying resistance $R_{cap}(t)$, which, according to the physiological demands, in the lower panel is concretized into a combination of two resistances and a compliance. The resistance R_4 might represent leakage by shunts outside the measured volume.

V_0 and V_1 can be considered as the aortic and the ankle pressure respectively. It appears that this combination of resistors $R_2..R_4$ and capacitor C_2 enables to comply with the demands: C_2 ensures that the capillary resistance is small, immediately after releasing the pressure, and grows gradually when the end situation is approached. In normal (healthy) situations R_4 will be large. Explicit expression for resistances and compliances were given by Westerhof [13] and Avolio [14], starting from Poiseuille's Law. He also gives an expression for the inductance L, which is not used in the present model.
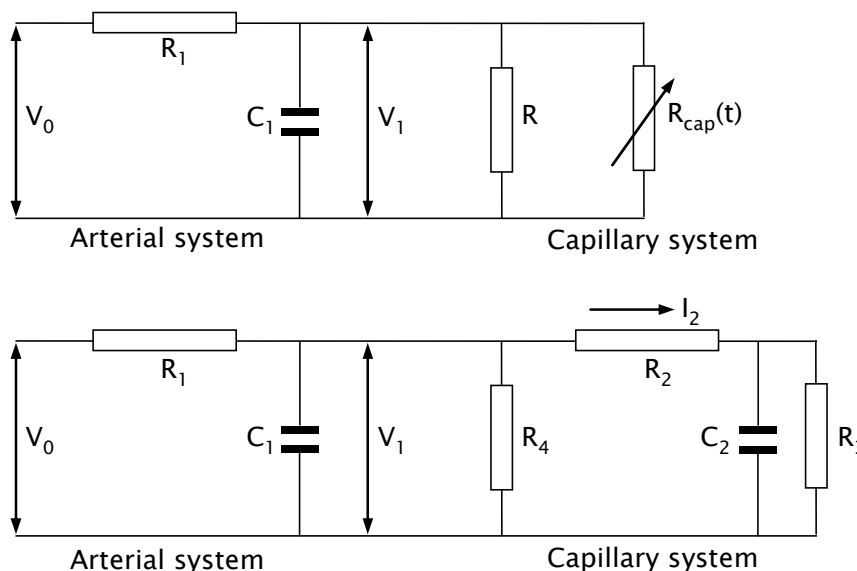

Figure 5.2. The PORH model. Upper panel: the capillary system is represented by a time-varying resistance $R_{cap}(t)$, parallel to a resistance representing possible extra-capillary leakage shunts. Lower panel: the complete model, with $R_{cap}(t)$ represented by a combination of resistances and a compliance, and with the arterial part (R_1, C_1) and the capillary part (R_2, R_3, R_4, C_2). I_2 denotes the measured current. Normally R_4 is large.

The exact solution for the flow current I_2 through resistance R_2, which is measured during the LDF experiment, can be derived using the standard approach for a response to a stepwise changing input signal, to be:

$$I_2 = \frac{Q_{end}}{C_2 R_3} \left[1 + \frac{1}{p_2 - p_1} \left\{ \left(C_2 R_3 p_1 p_2 - p_2 \right) \exp(-p_1 t) - \left(C_2 R_3 p_1 p_2 - p_1 \right) \exp(-p_2 t) \right\} \right] \quad (5.1)$$

where

$$Q_{end} = \frac{C_2 R_3 R_4 V_0}{R_4 (R_1 + R_2 + R_3) + R_1 (R_2 + R_3)} \quad (5.2)$$

and p_1 and p_2 are the real roots of the equation

$$a_2 p^2 + a_1 p + a_0 = 0 \quad (5.3a)$$

with

$$a_0 = \frac{R_1 + R_2 + R_3}{C_2 R_3} \quad ; \quad a_1 = -\left(R_1 + R_2 + \frac{R_1 C_1 (R_2 + R_3)}{C_2 R_3} \right) \quad ; \quad a_2 = R_1 R_2 C_1 \quad (5.3b)$$

From t = 0 (release of the occlusion) the value of I_2 will start from zero, while for t→∞ the value of I_2 will approach the "resting flux" value given by

$$I_{2,rest} = \frac{Q_{end}}{C_2 R_3} \quad (5.4)$$

In normal physiologically relevant situations, the two roots p_1 and p_2 appear to be positive and have different values. The parameters p_1 and p_2 can be seen as inverse characteristic times: $p_1 = \tau_1$ and $p_2 = 1/\tau_2$. In case these times are rather different, one of the exponentials in eq. 5.1 will still be about unity, while the other is already decreasing from 1 to zero. Then the function I_2 will tend to behave as a (1-exp)-increase from zero, followed by an exponential decrease to the end value (resting flow).

In order to get some more insight in the behaviour of the flow, we first assume that R_4 is much larger than R_2 and R_3. This implies that no large shunts outside the capillary bed are present. In that case the resting flow current $I_{2,rest}$, given in eqs. 5.2 and 5.4, will read

$$I_{2,rest} = \frac{V_0}{R_1 + R_2 + R_3} \quad (5.5)$$

Further, we assumed that the arterial subsystem is much faster developing in time than the capillary subsystem. This implies that we may treat both

sub-circuits as being independent. Then the solution can be described with the function:

$$I_2 = I_{2,rest} \left[1 - \exp(-\frac{t}{\tau_1}) \right] \left[1 + (\rho_M - 1).\exp(-\frac{t}{\tau_2}) \right] ,$$ (5.6)

$$\tau_1 = R_1 C_1 \quad ; \quad \tau_2 = C_2 \frac{R_2 R_3}{R_2 + R_3} \quad ; \quad I_{2,rest} = \frac{V_0}{R_2 + R_3} \quad ; \quad \rho_M = \frac{R_2 + R_3}{R_2}$$ (5.7)

with τ_1 and τ_2 as the time constants of the arterial and capillary part respectively, $I_{2,rest}$ as the resting flow when the stable situation has returned (with a value different from eq. 5.5), and ρ_M as the ratio of the maximum flow of the capillary part (at t = 0) and the resting flow (both above the biological zero level). In Figure 5.3 the two contributing parts are sketched. In the Figure, A and C denote the arterial and the capillary parts, respectively (note the two different ordinate scales). The two factors between brackets in eq. 5.6 describe the flux increase due to vasodilatation and the return to the resting flux respectively.

The ρ_M-ratio in eq. 5.7 does not necessarily correspond to the actual maximum value of the functions. Especially when $\tau_1 \approx \tau_2$ the difference between the two values may be large. This actual maximum cannot be calculated analytically from eq. 5.6.

The value for $I_{2,rest}$, as given in eq. 5.7, has been obtained under the condition that $\tau_1 << \tau_2$, which means that the effect of R_1 on the resting flux value has been masked. This can be corrected for by adding R_1 to $R_2 + R_3$ in the denominator:

$$I_{2,rest} = \frac{V_0}{R_1 + R_2 + R_3}$$ (5.8)

which might result in a better approximation (see also eq. 5.5).

In Figure 5.4 some hypothetical numerical results for $I_{2,rest}$, calculated with the exact solution and with the approximation are compared, for τ_1 / τ_2 = 1/5, 1/9 and 10/5 respectively. It is seen that the approximation in eqs. 5.6-7), with or without correction as in eq. 5.8, resembles the exact solution fairly well, even in cases where $\tau_1 << \tau_2$ is not valid any more. From the Figure, it is seen that a typical pattern for a "healthy" response (fig. 5.4a, b) is obtained when τ_1 is small compared to τ_2, which indicates that the impedance of the arterial system is (much) less than that of the capillary system. When the impedance of the arterial system increases (the "disease" case), the overflow will diminish and ρ_M will decrease to unity (fig. 5.4c).

We applied the functions given in eqs.(5.1-5) and (5.6-8) to fit the experimental values. The fitted parameters are: τ_1, τ_2 and ρ_M. Also the starting point of the function (at the instant of cuff release) was included as an (optional) parameter. For the fitting procedure we rewrote eq. 5.1 into

$$I_2 = I_{2,rest}\left[1 - \rho_M . \exp(-t/\tau_1) + (\rho_M - 1).\exp(-t/\tau_2)\right] \qquad (5.9)$$

In doing so, for $\tau_1 << \tau_2$ both models in eqs. 5.1 and 5.6 show a similar behaviour for small times:

$$I_2 = I_{2,rest} . \rho_M \left[1 - \exp(-t/\tau_1)\right] \qquad (5.10)$$

When comparing eqs. 5.1 and 5.9, the parameter values τ_1, τ_2 and ρ_M, can be related to p_1, p_2, R_1, R_2, R_3, C_1, and C_2. In this study we used these three as the fitted parameters, since these values will have a direct correspondence to clinical measurements, and we did not calculate the resistance and compliance values themselves.

We applied as the fitting scheme: minimisation of χ^2 calculated from the squared differences between the measured values and the function values, summed over all points in the time region between its starting point and a chosen time point were the measured values have returned to the level of the resting flux values. This was done by repeated subsequent stepwise variation of the three parameters around their actual value. When a smaller χ^2-value appeared, the new parameter value was adopted and the parameter step was increased with a factor $\sqrt{2}$. If not, the parameter step was reduced with that factor. To avoid being trapped in local minima, dur-
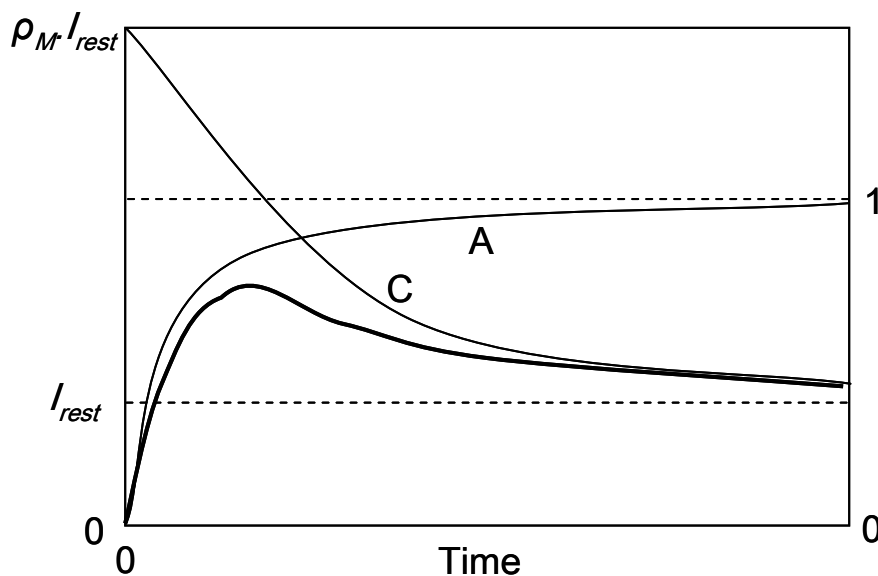

Figure 5.3. Sketch of the two functions in brackets of eq. (6): the Arterial part (A) and the capillary part (C) (including I_{rest}) on the right and left vertical scales, respectively. Thick line: full model (eq. 5.1).

ing the process we frequently multiplied the step values by a factor of 10 or 100, until eventually no change larger than 10^{-6}% in χ^2 was observed. To start the fitting process, initial parameter values could be inserted manually or using a coarse first parameter estimation based on the approximated model. Since for both models the maximum value cannot be calculated analytically, one might take the apparent maximum of the PORH-curve as the default starting value for ρ_M (the maximum value obtained in the limit that the smallest of τ_1 and τ_2 approaches zero (as indicated in fig. 5.3, see left scale)).

There is an option to include a Gaussian weighting filter $f_{corr}(t)$ for the points:

$$f_{corr}(t) = \exp\left[-(t/t_h)^2\right] \quad ; \quad t_h = t_{end}/2 \tag{5.11}$$

with tend as the end time point of the fit (all times are measured from the starting point). However, it turns out that applying this filter has only a slight effect on the resulting parameter values. This can be understood by realising that most significant contributions to χ^2 appear for small times t.

In some cases it is preferable to use some characteristic values, in addition to or instead of τ_1, τ_2 and ρ_M, like (fig. 5.1):

- *MF* (the apparent maximum of the model), or the ratio MF/I_{rest},

- t_{RF} (the time when the increasing curve crosses the extrapolated resting flux line),

- t_{MF} (the time at the apparent maximum), and

- t_{HF} (the time where the function – or the recording – has decreased half-way between the apparent maximum and the resting flux value.

Since it is not possible to calculate these values from the fitted models analytically, we calculated those values numerically. This was done using a parabolic 5-point fit through the 5 function points closest to the point of interest.

The program was written in Delphi-Pascal (the executable file is available from the authors).

5.3   Test measurements and Calculations

We analysed flux recordings from measurements performed on a wide range of microvascular conditions, provided by 24 subjects: 7 with PAOD, 9 with Diabetes Mellitus (DM) and 8 healthy persons (control group). All

persons with PAOD had Fontaine class II-III disease and had an ankle-brachial index < 0.9. Those with DM fulfilled ADA criteria for type I or type 2 DM, and had normal ankle brachial index and toe pressures. The Diabetes group was included for comparison.

We used a laser Doppler perfusion flow monitor (Perimed Pf4001, Perimed AB, Järfälla, Sweden; bandwidth 20 Hz - 12 kHz), with a custom-made probe with a fibre separation of 250 µm, attached between the second and third metatarsals of the subject's right foot, using a double-side adhesive ring. The monitor's signal processing calculates the zeroth and first moments, M_0 and M_1, of the frequency power spectrum $S(\omega)$ of the measured AC-signal $f(t)$:

$$M_n = \int_{\omega 1}^{\omega 2} \omega^n . S(\omega) . d\omega \quad ; \quad n = 0,1 \tag{5.12}$$

with ω_1 and ω_2 as the bandwidth limits given above. This calculation is done in the time domain, and corresponds to the zero-time autocorrelation values of the signal and its derivative respectively [15]. From $M_1(t)$ the Perfusion Flow is obtained after division (normalisation) with the square of the total reflection from the sample. $M_0(t)$ can be considered as a measure for the concentration of moving scattering particles (red blood cells). In this study, we did not use this function. A PC equipped with a data-acquisition subsystem recorded the analogue outputs of the monitor at a rate of 40 Hz. The data files were processed for conversion from mV to PU (perfusion units) by division with the gain factor of the instrument (10 mV/PU). Afterwards, the data were averaged over 40 samples to remove heart beat fluctuations. This resulted in data at 1 sec intervals.

The measurements were performed with the patient in the supine position, and the foot at 10 cm above heart level. The arterial occlusion was performed with a rapid cuff inflator (E-20 rapid cuff inflator and AG-101 air source, D.E. Hokanson, Bellevue, WA, USA) and a cuff of 18 cm around the thigh, above the knee. Before occlusion, we allowed for 30 minutes of acclimatisation time. The recording sessions started with 15 min of resting flux recording, followed by an occlusion of 3 min. The release of the cuff was done with the cuff deflator, as fast as possible (1-2 seconds), and the hyperaemia response was recorded for 15 min, to allow the flow to return to the resting value.

5.4   Results and Discussion

From the series of measurements, we show some typical examples in Figure 5.5, from a typical healthy subject and from a PAOD-patient. We also
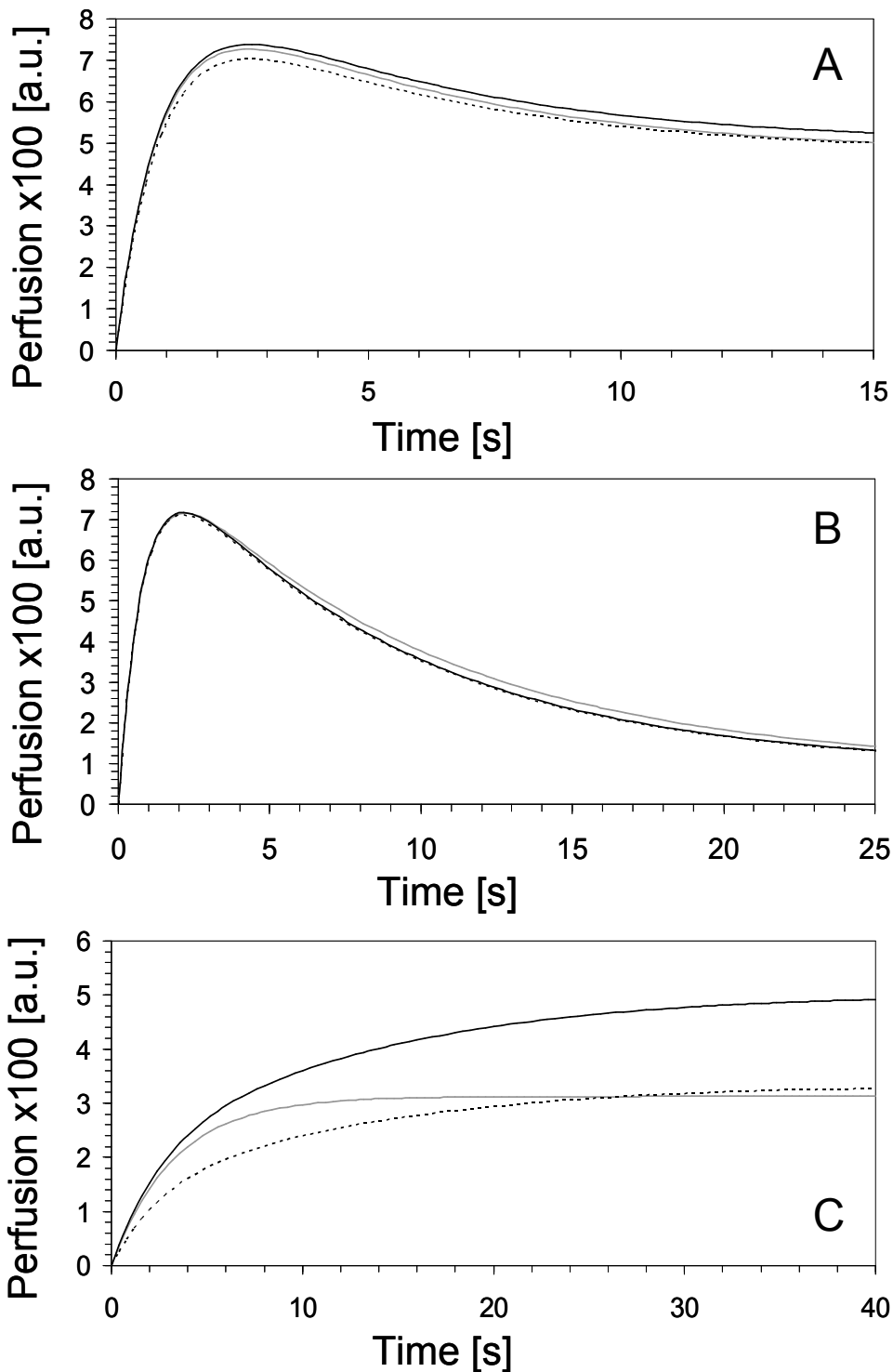
Figure 5.4. Numerical comparison of the exact model eq. 5.1 (black line) and the approximations eqs. 5.6-7 (gray line) and eqs. 5.6-8 (dotted line), for the situations (a), (b) and (c): R_1 = 1, 1 and 10; R_3 = 10, 100 and 10 respectively. Other parameters: V_0 = 1; R_2 =10; R_4 =100; C_1 = 1; C_2 = 1 (thus τ_1 = 1, 1 and 10; τ_2 = 5, 9 and 5 respectively). Units of: R: Ns/m^5, C: m^5/N; and V: Pa. The approximation resembles the exact model quite well, provided the arterial sub-model has a much shorter characteristic time than the capillary sub-model.

show the fit by the two models. The resulting parameter values are listed in Table 5.1. It is seen that with the healthy persons the two models and the values of their parameters are similar. However, for the patient group the curves do seem to coincide, but at the expense of very different parameter values, which means that here the values obtained for the approximated model are not realistic. This is connected with the assumptions made when introducing the approximation model: only valid when $\tau_1 << \tau_2$, which is met with the healthy cases only. The ratio of τ_2 and τ_1 was al ways larger than 1 and frequently larger than 10 for the healthy persons, but varied between 0.2 and 10 for the diseased persons.

Figure 5.6 shows the differences in characteristic times over the three groups, as obtained with eq. 5.1. The error bars are quite large (probably due to the limited amount of subjects). Especially the groups of PAOD-patients and Controls show large significant differences. The characteristic times of the patient group are much longer, probably due to the decrease of elasticity and/or increase in resistance of the arterial and the capillary system, or the disturbed endothelium-dependent vasodilatation in the patient group. All control subjects show a very rapid, almost instantaneous, increase in flow after releasing the occluding cuff.

We also included in the figure the ratio of the areas between the measured curve and the extrapolated resting flux line for the time after the starting point (the point of cuff release) and before that point. This was done by calculating the differences between the resting-flux points and the points of the measured curve, and add these differences over the two time periods indicated. This ratio of Reactive Hyperaemia versus Occlusion might indicate how the oxygen debt, created during the occlusion period, is paid off during the Reactive Hyperaemia period. The values show that for healthy persons (the control group) and the PAOD-patients this ratio is below and above unity respectively. Values for the diabetes mellitus patients resemble the Control group values. This point needs further investigation.

When comparing the strength of the PORH-signal, the ratio of the apparent maximum flux and the resting flux might be important. These ratios are 3.1 ±0.6 (SD), 5.8 ±4.8, and 3.2 ±2.7, averaged over the PAOD, DM, and healthy groups respectively. This indicates that this ratio cannot be used to discriminate between groups.

5.5   Discussion and Conclusions

We showed that using a simple two-stage model for the PORH-reaction we can explain differences in the recordings between groups of PAOD- and DM- patients and healthy persons. Although the model might be too simple

to explain the full physiological details of the PORH-phenomenon, it provides a convenient way to calculate characteristic values of times and signal strengths, which is of great importance when comparing recordings of individual persons or groups.

Table 5.1. Model parameters for a typical healthy person and a typical PAOD-patient.

Person	Model	$\tau_1(s)$	$\tau_2(s)$
Healthy (see Fig. 5.5a)	Exact: eq. 5.1	4.6	81.2
	Approx: eq. 5.6	4.7	81.2
PAOD-patient (see Fig. 5.5b)	Exact: eq. 5.1	80	86.1
	Approx: eq. 5.6	314	114
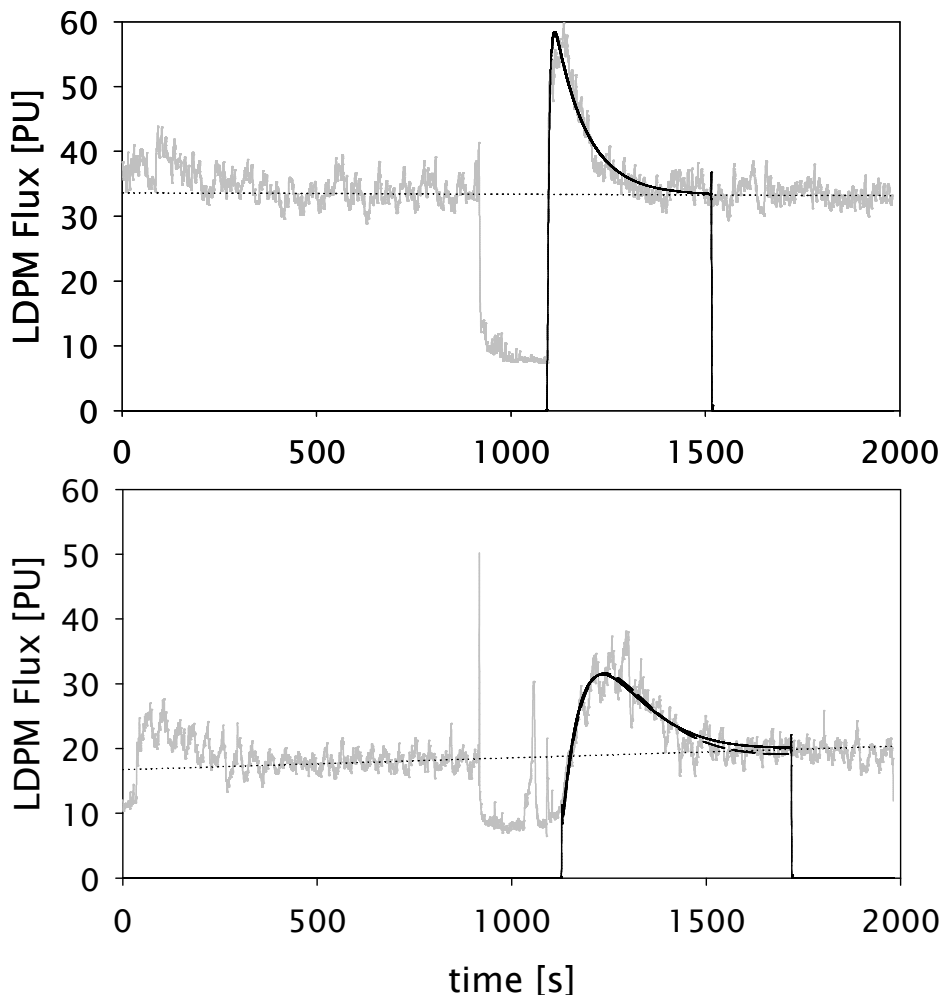
Figure 5.5. Analysis of two typical PORH-recordings, from a healthy person (a) and a PAOD-patient (b). Typical differences are: (very) fast vs. slow start after releasing the cuff, and fast vs. slow recovery towards normal resting flow values Fits are performed between the vertical lines. Nearly horizontal line RF: Resting flow and extrapolation. The arrows indicate the time where the model fit begins. In (a) both models coincide; in (b): exact model and approximation: lower and upper curve.

Therefore, we would like to propose this model as a method towards quantification of laser Doppler perfusion signals, to enable interpersonal comparisons, even with different instruments or between different researchers. The model may improve the discrimination between the PORH-responses of PAOD patients and controls, compared to the conventional use of single-curve characteristics. It may then transform the so-far limited use of LDF-PORH manoeuvres in clinical practice and provide a more convenient clinical tool. The model is developed to describe whole-limb ischemia cases, and therefore is probably less applicable in other Reactive Hyperaemia cases.

The model can be used on all recordings of PORH-signals, provided enough time before the occlusion and after the return to the resting flux signal is present to record the signal to define the resting flux trend line. Frequently it is necessary to first remove artificial spikes or other artefacts from the signal. Moreover, sometimes also a slow pseudo-sinusoidal vasomotion contribution is present (frequencies smaller than about 0.1 Hz). The analysing program we developed is capable of dealing with all these effects.

Finally, we would like to note that this contribution has the objective to focus on the physical aspects of the proposed model. We therefore did not discuss here endothelial function and related physiological or clinical questions in detail. This could be the subject of following dedicated contributions.
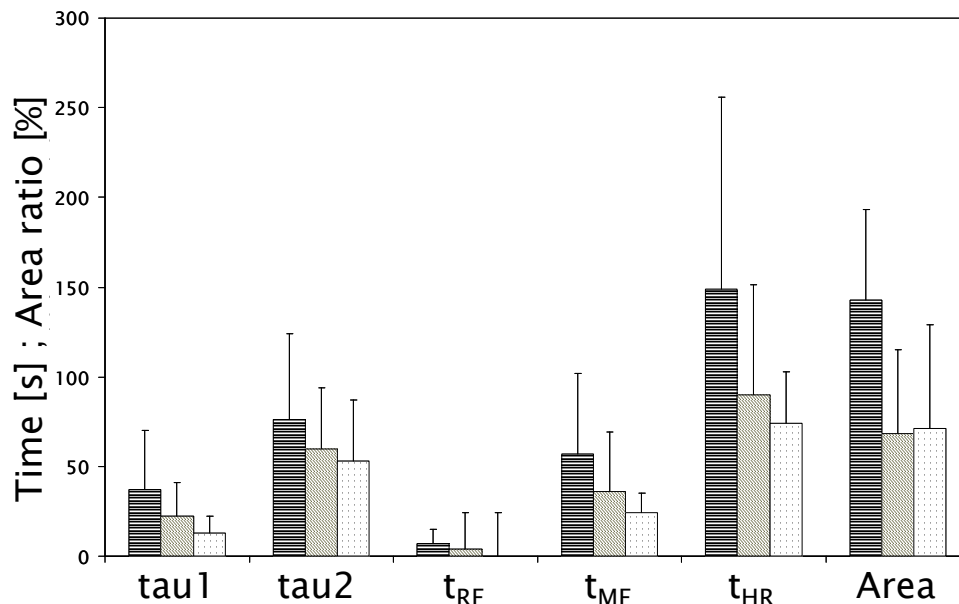

Figure 5.6. Comparison of characteristic times for the three groups with eq. 5.1 (left: PAOD, middle: Diabetes Mellitus, right: Healthy persons). τ_1, τ_2 are: characteristic times in eqs. 5.1-6; t_{RF}, t_{MF}, t_{HR} are: time to resting flux value, time to maximum flux value, and time to half return to resting flux after maximum, respectively, all measured from time of cuff release. Also indicated: Ratio of areas between measured data and extrapolated resting flux, for occlusion period and reactive hyperaemia period vs. occlusion period. Error bars indicate the standard error of the mean.

5.6   References

1.   Andreassen, A. K., Kvernebo, K., Jorgensen, B., Simonsen, S., Kjekshus, J., and Gull-estad, L., Exercise capacity in heart transplant recipients: relation to impaired endothe-lium-dependent vasodilation of the peripheral microcirculation, Am.Heart J., vol. 136, no. 2, pp. 320-328, Aug.1998.

2.   Wahlberg, E., Olofsson, P., Swedenborg, J., and Fagrell, B., Effects of local hyperemia and edema on the biological zero in laser Doppler fluxmetry (LD), Int.J.Microcirc.Clin.Exp., vol. 11, no. 2, pp. 157-165, May1992.

3.   Del Guercio, R., Leonardo, G., and Arpaia, M. R., Evaluation of postischemic hyperemia on the skin using laser Doppler velocimetry: study on patients with claudicatio intermit-tens, Microvasc.Res., vol. 32, no. 3, pp. 289-299, Nov.1986.

4.   Kvernebo, K., Slasgsvold, C. E., and Stranden, E., Laser Doppler flowmetry in evaluation of skin post-ischaemic reactive hyperemia. A study in healthy volunteers and atheroscle-rotic patients, J.Cardiovasc.Surg.(Torino), vol. 30, no. 1, pp. 70-75, Jan.1989.

5.   Frank, O., Die Grundfurm des arteriellen Puls, Zeitschr, F.Biologie, no. 37, pp. 483, 1899.

6.   Westerhof, N., Elzinga, G., and Sipkema, P., An artificial arterial system for pumping hearts, J.Appl.Physiol, vol. 31, no. 5, pp. 776-781, Nov.1971.

7.   Burattini, R. and Gnudi, G., Computer identification of models for the arterial tree input impedance: comparison between two new simple models and first experimental results, Med.Biol.Eng Comput., vol. 20, no. 2, pp. 134-144, Mar.1982.

8.   Geertsema, A. A., Rakhorst, G., Mihaylov, D., Blanksma, P. K., and Verkerke, G. J., De-velopment of a numerical simulation model of the cardiovascular system, Artif.Organs, vol. 21, no. 12, pp. 1297-1301, Dec.1997.

9.   Ferrari, G., Nicoletti, A., De Lazzari, C., Clemente, F., Tosti, G., Guaragno, M., Mimmo, R., Ambrosi, D., and Gorczynska, K., A physical model of the human systemic arterial tree, Int.J.Artif.Organs, vol. 23, no. 9, pp. 647-657, Sept.2000.

10.   Humeau, A., Saumet, J. L., and L'Huillier, J. P., Simplified model of laser Doppler signals during reactive hyperemia, Med.Biol.Eng. Comput., vol. 38, no. 1, pp. 80-87, Jan.2000.

11.   Smye, S. W. and Bloor, M. I., A single-tube mathematical model of reactive hyperemia, Phys.Med.Biol., vol. 35, no. 1, pp. 103-113, Jan.1990.

12.   Wilkin, J. K., Cutaneous reactive hyperemia: viscoelasticity determines response, J.Invest Dermatol., vol. 89, no. 2, pp. 197-200, Aug.1987.

13.   Westerhof, N. and Elzinga, G., Fluid mechanics for arterial functions, Nederlands Tijdschrift voor Natuurkunde., vol. 41, no. 17, pp. 267-273, Nov.1975.

14.   Avolio, A. P., Multi-branched model of the human arterial system, Medical.& Biological Engineering.& Computing., vol. 18, no. 6, pp. 709-718, Nov.1980.

15.   Nilsson, G. E., Signal processor for laser Doppler tissue flowmeters , Medical and Bio-logical Engineering and Computing, vol. 22, pp. 343-348, 1984.